Mohammad Kamruzzaman Talukder
PhD, Assistant Professor
Department of Civil Engineering
East West University, Dhaka
Bangladesh
mktalukder@ewubd.edu
0009-0003-4502-2609

APPLICATION OF C++ COMPUTER PROGRAMMING TO INCREMENTAL STRESS UPDATE PROCEDURE FOR NUMERICAL IMPLEMENTATION OF THE MODIFIED CAM-CLAY CONSTITUTIVE MODEL – A CONTRIBUTION TO THE TEACHING OF GEOMECHANICS

DOI: doi.org/10.55302/SJCE2514121kt

Teaching the computation of soil stress-strain responses presents a significant challenge in geomechanics education. Over the past decade, modern programming languages, particularly C++, have been integrated into the curricula of undergraduate and graduate engineering programs to facilitate the application of numerical methods in geomechanics. Among the various models used to predict the nonlinear response of soil to monotonic stress, the modified Cam-clay (MCC) soil plasticity model is widely recognized and taught in geomechanics courses at engineering institutions worldwide. However, the numerical implementation of the MCC model using contemporary programming languages within the framework of the Invariants of Stress Tensor is not extensively documented in publicly available resources. This study addresses this gap by numerically solving the MCC model through the Invariants of Stress Tensor, employing the Gauss Elimination method and the Incremental Stress Update Method. Additionally, a flow chart is included to illustrate the implementation process.

Keywords: Modified Cam-clay, Stress path, Gauss elimination, yield surface, Incremental Stress Update procedure, plastic strain, shear strain, volumetric strain.

1. INTRODUCTION

In this study, the modified cam-clay (MCC) plasticity model of critical state soil mechanics is selected for the stress-strain response and

stress path computations. Computer C++ programming is used to implement the stress-strain computation algorithms for the MCC model that can take into account soil elastoplasticity. The MCC model is implemented using the incremental stress update (ISU) method, which can solve a system of linear algebraic equations relating stress increments to strain increments.

The ISU method used by Hashiguchi et al. (Hashiguchi, Saitoh, & Okayasu, 2002) is implemented in the study for numerical test of the MCC model. In the ISU method, an incremental strain vector is calculated by solving elastoplastic constitutive relations of the MCC model with Gauss elimination technique (Hashiguchi, Saitoh, & Okayasu, 2002). By multiplying the stress-strain matrix with the incremental strain matrix, incremental stresses are directly updated once the MCC model's yield criterion has been met. In this procedure, the approximate solution for the stresses diverge from the analytical solution after a number or stress increments. In the study, the linear algebraic equations are solved using Gauss elimination technique (GET) for unknown stress and strain values. Stress-strain response and stress path computed in the study are compared with PLAXIS numerical triaxial test results and analytical closed form solutions. The stress-strain response and stress path response calculated with the ISU method compares well with the PLAXIS simulation results and analytical solution. This study uses a few soil parameters that can be obtained from straightforward geotechnical drained and undrained triaxial tests at a variety of working loads of interest rather than just loads at failure to accurately predict the stress-strain response. The C++ computer program is provided in the paper in order to facilitate the teaching and learning numerical methods in geomechanics at graduate schools across the world.

To fully comprehend how the study implemented the MCC elastoplastic model using the incremental ISU method, we need to review literature on non-linear elasto-plastic stress analysis. The literature include concepts of general elasticity and plasticity of soils.

1.1 MODELING OF GEOMATERIAL RESPONSE

Stress-strain response of geomaterials can be obtained by experimental methods but experimental methods are time consuming and at times can be inaccurate because of sample disturbances. Soil constitutive modeling is a branch of geomechanics, where numerical methods are used to accurately describe experimentally observed stress-strain responses, for example, irreversible deformation and yield phenomena of soils and rock under both static and dynamic loading conditions. However, using mathematical relations to predict the response of geomaterials under all possible loading conditions is not always possible The following requirements must be met for a numerical model of the stress-strain response of geomaterials to be useful.

The material response model should be able to predict the material behavior for all stress and strain paths and not just a single class of paths (for example, axial symmetry or pure shear). A small number of straightforward geotechnical laboratory tests should be enough to estimate the model's parameters. Elastoplastic nonlinear soil response to loading and unloading conditions (stress history) should be predicted by the model.

Many of the aforementioned characteristics of material models have been successfully described using elasto-plasticity models based on critical state formulation. Soil hardening, softening, and stress history are all included in the MCC, a critical state-based model with 3D stress and strain calculations. The MCC model requires few model parameters which can be directly obtained from standard oedometer and conventional tri-axial compression tests.

1.2 LINEAR ELASTIC MATERIAL

Stress-strain response of isotropic linear elastic materials are described by the following relationships:

Incremental volumetric strain in a soil element,

$$d\varepsilon_v = \frac{1}{K'} dp \quad (1)$$

where, K'=bulk modulus of soil

dp = incremental mean effective pressure on a soil element

Incremental shear strain

$$d\varepsilon_s = \frac{1}{3G} dq \quad (2)$$

where, G = shear modulus of soil and ε_s is the shear strain.

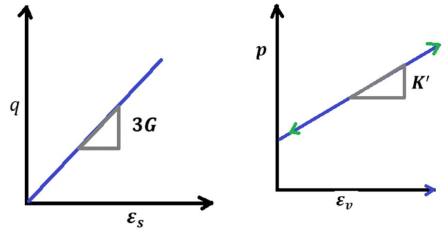

a) shearing (b) Isotropic compression and swelling

Figure 1: Behavior of isotropic linear elastic material

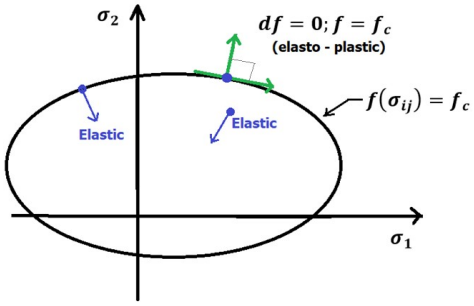

Figure 2: Schematic yield surface for a perfectly plastic material response to biaxial loading

In matrix form

$$\begin{bmatrix} d\varepsilon_v \\ d\varepsilon_s \end{bmatrix} = \begin{bmatrix} \frac{1}{K'} & 0 \\ 0 & \frac{1}{3G} \end{bmatrix} \begin{bmatrix} dp \\ dq \end{bmatrix} \quad (3)$$

1.3 INELASTIC SOIL MATERIAL

Soils are considered inelastic materials because they only behave elastically for strains typically less than 10^{-5}. For most soils, the elastic response is only a small part of the overall deformation and the response can be significantly different in relation to that predicted by elastic theory. Inelastic soils exhibit the following features:

Elastic and plastic (i.e., inelastic) deformation components of total strain are independent

$$\boldsymbol{\varepsilon^t = \varepsilon^e + \varepsilon^p} \quad (4)$$

1.4 YIELD FUNCTIONS FOR INELASTIC MATERIAL

A yield function mathematically expresses every possible combination of biaxial or triaxial stresses that can cause inelastic material to yield. The yield surface of an elastoplastic material is fixed in stress space. First, let us look at the yield surface below in biaxial stress space.:

$$\boldsymbol{df = 0; f = f_c} \quad (5)$$

$$\boldsymbol{f(\sigma_{ij}) = f_c} \quad (6)$$

In general the initial yield function for stress-strain response of elast0-plastic material can be described as below:

$$\boldsymbol{f(\sigma_{ij}) = f_c} \quad (7)$$

For all stress states within the yield surface the yielded material will behave elastically. The loading condition for elastic response is given by

$$\boldsymbol{f < f_c} \quad (8)$$

If the stress state coincides with the yield locus then and only then, plastic strain will occur. Thus, the loading condition for plastic behavior is given by:

$$\boldsymbol{f = f_c} \quad (9)$$

$$\boldsymbol{df = \frac{\partial f}{\partial \sigma_{ij}}} \quad (10)$$

If a stress path originates from the yield locus, the loading condition is given by;

$$\boldsymbol{f = f_c} \quad (11)$$

$$\boldsymbol{df = \frac{\partial f}{\partial \sigma_{ij}} d\sigma_{ij} < 0} \quad (12)$$

1.5 FLOW RULE AND HARDENING LAW

The ratio of incremental plastic shear strain to incremental plastic volumetric strain is used to express the direction of an incremental plastic strain vector. The relationship between the state of stress and the direction of the vector of plastic strain is known as flow rule. A flow rule defines the relationship between the net increment of the plastic strain increment $\boldsymbol{\varepsilon_{ij}^p}$, and the present state of stress $\boldsymbol{\sigma_{ij}}$.

Increased yield stress level due to plastic straining is called material hardening. The relationship between the increase in the yield stress and plastic strain is known as hardening law.

$$\boldsymbol{g\left(\sigma_{ij}, \varepsilon_{ij}^{p}\right) = 0} \quad (13)$$

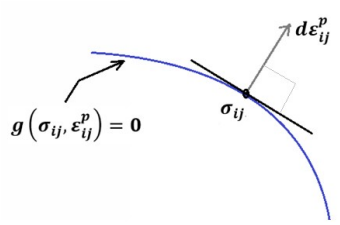

Figure 3: Representation of flow rule

Incremental plastic strain is expressed (Chen & Mizuno, 1990) below

$$\boldsymbol{d\varepsilon_{ij}^{p} = d\lambda \frac{dg}{d\sigma_{ij}}} \quad (14)$$

In above equation $\boldsymbol{d\lambda}$ is a positive scalar proportionality quantity which is dependent on the state of stress and loading history. If the plastic potential surface and yield surface coincide with each other, then, it is $\boldsymbol{f = g}$, the flow rule is called the associated flow rule; otherwise it is the non-associated type. It can be seen in the equation of flow rule, the direction of the plastic strain increment vector $\boldsymbol{d\varepsilon_{ij}^{p}}$, is normal to the plastic potential surface g at the current stress point $\boldsymbol{\sigma_{ij}}$ which is known as normality condition. Normality rule is more appropriate for clay and less so for sand.

1.6 PLASTIC WORK

Plastic work done per unit volume of a deformable elasto-plastic material during a strain increment $d\varepsilon$ is given by;

$$\boldsymbol{dW = \sigma_{ij} d\varepsilon_{ij}} \quad \textbf{(15)}$$

where, $d\varepsilon_{ij}$ is the total strain increment. This consists of both elastic and plastic components. It can be decomposed as;

$$\boldsymbol{d\varepsilon_{ij} = d\varepsilon_{ij}^{e} + d\varepsilon_{ij}^{p}} \quad (16)$$

Therefore, $\boldsymbol{dW}$ is given by

$$\begin{aligned} \boldsymbol{dW} &= \boldsymbol{\sigma_{ij}}\left(\boldsymbol{d\varepsilon_{ij}^{e} + d\varepsilon_{ij}^{p}}\right) \\ &= \boldsymbol{\sigma_{ij} d\varepsilon_{ij}^{e} + \sigma_{ij} d\varepsilon_{ij}^{p}} \\ &= dW^{e} + dW^{p} \end{aligned} \quad (17)$$

Where, dW^{e} is the recoverable elastic energy and dW^{p} is the plastic work.

1.7 CONCEPT OF CRITICAL VOID RATIO

When a loose sand or normally consolidated clay is sheared, it passes through progressive states of yielding before failure. That is, plastic deformations occur as the stress path passes through multiple yield surfaces. The material will continue to yield until it reaches a critical void ratio, at which point the void ratio won't change during subsequent shearing. That is, during shearing, the material reaches a point where the packing of the particles is such that there is no change in volume (Wood, 1991). This particular void ratio is called the critical void ratio. This can be considered as the critical state of the material (Wood, 1991). At the point when a dense sand or heavily overconsolidated clay is sheared, it reaches a peak stress and afterward reaches a residul stress. It is hown in figure below that, the material volume initially decreases, then dilates until the volumetric strain reaches a constant value which corresponds to its critical value.

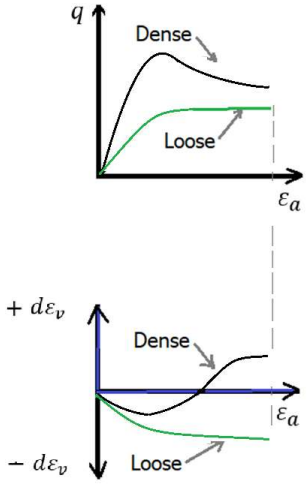

Figure 4: Stress-strain response of soil

1.8 SOIL YIELD SURFACE BASED ON THE CRITICAL STATE COCNCEPT

Effective confining stress (p), deviatoric stress (q), and void ratio (e) were among the crucial parameters utilized in the creation of critical

state models. With respect to cylindrical triaxial compression, those parameters are described below:

For the axissymmtery triaxial condition, $\boldsymbol{\sigma_1 = \sigma_2}$ and $\boldsymbol{\varepsilon_1 = \varepsilon_2}$; hence the work done on a test specimen per unit volume is given by

$$dW = \sigma_1 d\varepsilon_1 + \sigma_2 d\varepsilon_2 \quad (18)$$

$$dW = \left(\frac{\sigma_1 + 2\sigma_3}{3}\right)(d\varepsilon_1 + 2d\varepsilon_3) + (\sigma_1 - \sigma_3)\frac{2}{3}(d\varepsilon_1 - d\varepsilon_3) \quad (19)$$

Now let us define the above parameters as given below:

$$p = \frac{\sigma_1 + 2\sigma_3}{3} = \frac{J_1}{3}$$
$$= \text{mean effective stress}$$

Deviatoric stress of shear stress is given by;

$$q = \sigma_1 - \sigma_3 = \sqrt{2J_{2D}} \quad (20)$$

Volumetric incremental strain is given by;

$$d\varepsilon_v = d\varepsilon_1 + 2d\varepsilon_3 \quad (21)$$

Incremental shear strain is given by;

$$d\varepsilon_s = \frac{2}{3}(d\varepsilon_1 + d\varepsilon_3) \quad (22)$$

Therefore the quantitu dW can be written:

$$dW = pd\varepsilon_v + qd\varepsilon_s \quad (23)$$

The below figure shows typical results of undrained triaxial tests on NC samples. As it can be seen, the stress paths are geometrically similar and the ultimate states Q1, Q2, Q3, etc, lie on a straight line on the q-p plot. The same states are observed to lie on a curve which is similar to the isotropic consolidation line on e-p plot (Desai & Siriwardane, 1984).

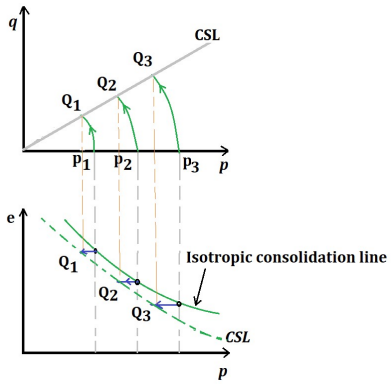

Figure 5: Undrained stress paths for normally consolidated clay

Typical results of stress paths in draned triaxial tests on NC clay sample are shown in Figure 6 as a function of deviatoric stress q, mean confining pressue p and void ratio.

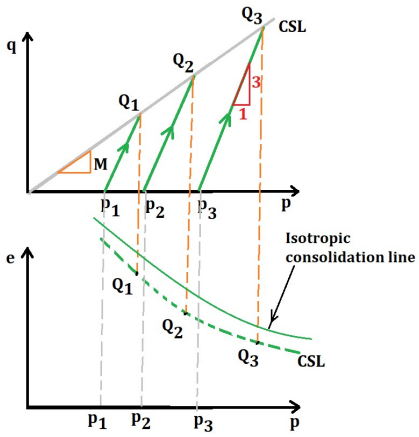

Figure 6: Drained stress paths for normally consolidated clay

Figure 6 demonstrates that, the ultimates states (failure points) also lie on the critical state (critical void ratio) line. The slope of the CSL on q-p plot is M and it is a material parameter. It is noted in Figure 5 and Figure 6 that material failure can happen when the material reaches the CSL.

1.9 STATE BOUNDARY SURFACE IN 3D SPACE OF DEVIATORIC STRESS-MEAN CONFINING PESSURE-VOID RATIO

Figure 7 shows a schematic representation of soil response as a function of sear stress q, confining stress p and void ratio e (Roscoe K. H., 1970; Roscoe, Schofield, & Wroth, 1958). Two surfaces ABCD and BCC'B' intersect at the CSL.

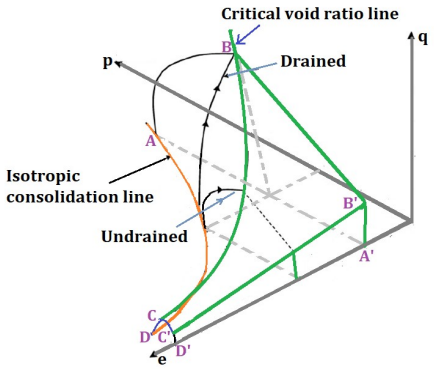

Figure 7: Isometric view of yeild surface

The material can undergo any state (q, p, e) below the two surfaces ABCD and BCC'B'. States of wet and isotropic normally consolidated (or loose) soil lie below the surface ABCD, whereas dry and overconsolidated (or dense) soil lie below BCC'B' surface. Before the material response reach CSL, it passes through states of yielding. The material hardens as it moves from one state of yileding to another. Subsequent yileding can lead to a state when the material is sheared without changing its volume. Figure 8 shows a projection of the crical void ratio line (or critical state line CSL) on the $q-p$ space and the yield surfaces. The projection of critical void ratio line (Figure 7) is usually a straight line passing through the origin of $q-p$ plot (Figure 8). The projection of the state boundary surface form continuous curves and are referred to as yield surface, yield locus or yield cap shown in Figure 8.

Figure 8 shows that point A is within the yield surface on $q-p$ space and it is a combination of q and p. The soil will respond elastically to the combination of q and p stresses when all possible combinations are contained within the yield surface (point A in Figure 8). On the initial yield surface, point B represents a novel combination of q and p. The yielding of steel rebar under tensile stresses is analogous to the yielding of the soil at point B. The current yield surface expands so that the stress point (q and p) lies on the expanded yield surface (points C and D) and not outside the expanded yield surface in the event that any stress point (of q and p) tends to fall outside the current yield surface passing through point B. The soil responds elastoplastically when there are effective stress paths that connect the B, C, and D points directly.

Spherical, bullet and elliptical shapes are assumed to be yield surfaces of soils. A yield surface intersects the CSL at the critical point. For NC clay, yield surfaces exist only between the CSL and p axis. Continuation of these surfaces from the CSL the origin of q-p space is shown in dashed lines (Figure 8) in order to indicate a complete shape of the yield locus. The mean confining pressure corresponding to the intersecton of the yield locus and the p -axis is denoted by p_0. Each surface has its unique p_0 which defines the strain hardening response.

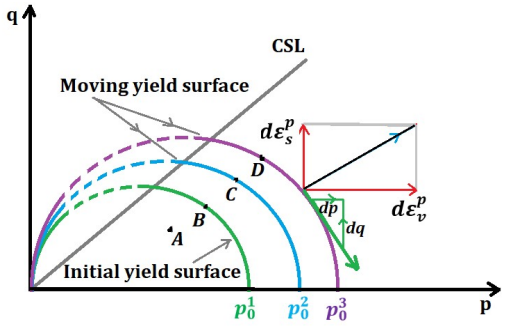

Figure 8: Yield locus in q-p space.

Soil response on $q-p$ plot is simulated by conventional triaxial tesst and that on $e-p$ space by one dimensional consolidation tests (Roscoe, Schofield, & Wroth, 1958). The numerical implementation of the MCC constitutive law within the framework of the critical state concept is the subject of the subsequent sections.

1.10 STRESS AND STRAIN PREDICTION BY THE MCC MODEL IN THREE DIMENSIONAL STATE OF STRESES

Let us consider the response of saturated clay to isotropic loading in $\boldsymbol{e-\ln(p)}$ plot as shown in Figure 9. Line AC is the virgin compression line while BD is the unloading line and DB is reloading line. Slope of AB is denoted by $\boldsymbol{\lambda}$ and slope of BD is denoted by $\boldsymbol{\kappa}$. Because of the elasto-plastic nature of soil response to the loading, the unloading path BD will not follow the AB loading line. Since the unloading path BD and reloading path DB are the same paths, they show elasic response (elastic incremental void ratio e^e). As shown in Figure 9, the vertical distance shows incremental plastic void ratio $\mathbf{e^p}$. Now, we can write change in void ratio during the loading-reloading cyclesas below:

$$\Delta e = e_A - e_B = \lambda(\boldsymbol{ln}p_B - \boldsymbol{ln}p_A) \quad (24)$$

$$\Delta e^e = e_D - e_B = \kappa(\boldsymbol{ln}p_B - \boldsymbol{ln}p_D) \quad (25)$$

$$\Delta e^p = \Delta e^t - \Delta e^e \quad (26)$$

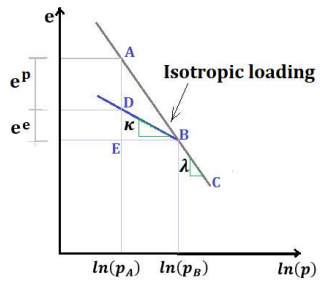

Figure 9: One dimensional consolidation response of OC clay on $\boldsymbol{e - \ln(p)}$ plot

Differentiating the above two relationships give us:

$$de = -\lambda \frac{dp}{p} \tag{27}$$

$$de^e = -\boldsymbol{\kappa} \frac{dp}{p} \tag{28}$$

$$de^p = de - de^e = -(\lambda - \boldsymbol{\kappa}) \frac{dp}{p} \tag{29}$$

where the superscript de^e denotes the recoverable incremental elastic void ratio and de^p is the irrecoverable plastic incremental void ratio. With compressive volumentric strain positive, we have;

$$d\varepsilon_v = -\frac{de}{1+e_0} = \frac{\lambda}{1+e_0}\frac{dp}{p} \tag{30}$$

Elastic component of the above volumetri strain is given by;

$$d\varepsilon_v^e = -\frac{de^e}{1+e_0} = \frac{\boldsymbol{\kappa}}{1+e_0}\frac{dp}{p} \tag{31}$$

According to the normality rule, incremental plastic strain vector $d\varepsilon_v^p$ is normal to the yield surface (Figure 8) at any point on the yield locus (Chen & Mizuno, 1990). Thus, ratio of the volumetric plastic strain vector $d\varepsilon_v^p$ to the plastic shear strain $d\varepsilon_s^p$ is given by;

$$\frac{d\varepsilon_v^p}{d\varepsilon_s^p} = -\frac{dp}{dq} \tag{32}$$

1.11 EQUATION OF THE YIELD LOCUS OF THE MCC MODEL

Let us define stress ratio

$$\eta = \frac{q}{p} \tag{33}$$

$$q = \eta p \tag{34}$$

$$dq = pd\eta + \eta dp \tag{35}$$

Slope of the yield curve at any point (p, q) on the yield surface (Figure 8) is given by;

$$\psi = -\frac{dq}{dp} \tag{36}$$

Substituting the value of ψ into equation (32), it is written

$$\frac{d\varepsilon_v^p}{d\varepsilon_s^p} = -\frac{dq}{dp} = -\psi \tag{37}$$

In equations (36) and (37), the sign of ψ is negative because, q decreases with an increment in p.

$$=> dq = -\psi dp \tag{38}$$

Substitution of equation (38) in to equation (35) results in the following expression;

$$pd\eta + \eta dp = -\psi dp \tag{39}$$

By rearranging, this can be written below (Desai & Siriwardane, 1984);

$$=> \frac{dp}{p} + \frac{d\eta}{\eta + \psi} = 0 \tag{40}$$

The above equation (40) defines a yield locus. Since all sucessive yield loci (hardening caps) are geometrically the same (Desai & Siriwardane, 1984), the slope of the hardening cap ψ is only a function of the stress ratio η. Therefore, an equation for the yield curve shown in Figure 8 is derived by integrating equation (40);

$$\int_{p_0}^{p} \frac{dp}{p} + \int_{0}^{\eta} \frac{d\eta}{\eta + \psi} = 0 \tag{41}$$

$$=> lnp - lnp_0 + \int_{0}^{\eta} \frac{d\eta}{\eta + \psi} = 0 \tag{42}$$

Equation (42) represents an yield curve which passes through a point $(p_0, 0)$ on p –axis; where p_0 is treated as the hardening parameter which is unique for any yield surface. Equation (42) canbe expressed in the following differential form:

$$\frac{dp}{p_0} - \frac{dp}{p} - \frac{d\eta}{\psi + \eta} = 0 \quad (43)$$

Inserting $p = p_0$ in equation (29), the following equation is written for incremental plastic void ratio;

$$de^p = -(\lambda - \boldsymbol{\kappa})\frac{dp_0}{p_0} \quad (44)$$

Substituting equation (43) into (44), it can be written;

$$de^p = -(\lambda - \boldsymbol{\kappa})\left(\frac{dp}{p} + \frac{d\eta}{\psi + \eta}\right) \quad (45)$$

Therefore, the plastic volumentric strain vector can be written:

$$d\varepsilon_v^p = \frac{de^p}{1+e} = \frac{\lambda - \kappa}{1+e}\left(\frac{dp}{p} + \frac{d\eta}{\psi + \eta}\right) \quad (46)$$

In the Cam-clay model it is assumed that

$$dW = Mpd\varepsilon_s \quad (47)$$

Using equation (23), it is written;

$$pd\varepsilon_v^p + qd\varepsilon_s^p = Mpd\varepsilon_s \quad (48)$$

Since there is no recoverable energy associated with shearing strain (Desai & Siriwardane, 1984),it is assumed that $\boldsymbol{d\varepsilon_s^e = 0}$. Substituting $\boldsymbol{d\varepsilon_s = d\varepsilon_s^p}$ into equation (48), it is writen;

$$\frac{d\varepsilon_s^p}{d\varepsilon_v^p} = \frac{1}{M - \eta} \quad (49)$$

Substituting equation (49) into equation (37), it is now written for the modified Cam-clay model,

$$\psi_c = M - \eta \quad (50)$$

In the above equation (50), the subscript $\boldsymbol{c}$ stands for the Cam-clay. In the MCC model the dissipated energy during plastic deformation is written:

$$dW = p\sqrt{\left(d\varepsilon_v^p\right)^2 + M^2\left(d\varepsilon_s^p\right)^2} \quad (51)$$

Using equations (47) to (51), it is written;

$$\frac{d\varepsilon_s^p}{d\varepsilon_v^p} = \frac{2\eta}{M^2 - \eta^2} \quad (52)$$

$$\psi_{cm} = \frac{M^2 - \eta^2}{2\eta} \quad (53)$$

where, the subscripts cm is used to idicate that the value of above ψ is for the MCC model.

Once ψ is substituted into equation (41) , the yield locus for the MCC model can be found by the integrations of equation (41);

$$\int_{p_0}^{p}\frac{dp}{p} = -\int_{0}^{\eta}\frac{d\eta}{\eta + \frac{M^2 - \eta^2}{2\eta}} \quad (54)$$

$$=> \ ln(M^2 + \eta^2) - ln(M^2) = -lnp + lnp_0 \quad (55)$$

$$M^2p^2 - M^2p_0p + q^2 = 0 \quad (56)$$

Equation (56) is the equation of an ellipse on $\boldsymbol{q}$ **-** $\boldsymbol{p}$ plot. From equation (30) and (46), it can be written that,

$$d\varepsilon_v^p = d\varepsilon_v - d\varepsilon_v^e = \left(\frac{\lambda - \kappa}{1 + e^0}\right)\frac{dp_0}{p_0} \quad (57)$$

$$=> \frac{\partial p_0}{\partial \varepsilon_v^p} = \frac{p_0(1 + e_0)}{\lambda - \kappa} \quad (58)$$

From equation (56), the yield function is expressed below;

$$f = M^2p^2 - M^2p_0p + q^2 = 0 \quad (59)$$

where, q is expressed in terms of 3D triaxial state of stresses

$$q = \sigma_1 - \sigma_3 \quad (60)$$

Stress invariants are introduced in the equation of yield surface f when 3D incremental plasticity computation is performed.

$$q = \sqrt{3J_{2D}} \quad (61)$$

where , $J_{2D} = \frac{1}{6}[(\sigma_{11} - \sigma_{22})^2 + (\sigma_{22} - \sigma_{33})^2 + (\sigma_{11} - \sigma_{33})^2] + \sigma_{12}^2 + \sigma_{23}^2 + \sigma_{31}^2$

The yield function can be written in terms of the stress invariants (Chen & Mizuno, 1990);

$$f = M^2 I_1^2 - M^2 I_1 I_{10} + 27 J_{2D} = 0 \quad (62)$$

where, $I_1 = 3p = (\sigma_{11} + \sigma_{22} + \sigma_{33})$ and I_{10} is the value of I_1 at the intersection of the yield surface with the I_1axis which is analogous to p_0 axis. The parameter I_{10} is a hardening paramter which depends on the plastic volumetric strain (Chen & Mizuno, 1990).

When soil yields, the stress point will be on the yield surface. It is expressed by;

$$f = f\left(p, q, p_0\left(\varepsilon_v^p\right)\right) \quad (63)$$

$$df = \frac{\partial f}{\partial q} dq + \frac{\partial f}{\partial p} dp + \frac{\partial f}{\partial \varepsilon_v^p} d\varepsilon_v^p = 0 \quad (64)$$

The normality rule for plastic deformation can be written as;

$$d\varepsilon_{ij}^p = \overline{d\lambda} \frac{\partial Q}{\partial \sigma_{ij}} \quad (65)$$

where, Q is the plastic potential and $\overline{d\lambda}$ is the scalar parameter of proportionality

$$d\varepsilon_{ij}^p = \overline{d\lambda} A_{ij} \quad (66)$$

$$A_{ij} = \frac{\partial Q}{\partial \sigma_{ij}} = \frac{\partial Q}{\partial p}\left(\frac{\partial p}{\partial \sigma_{ij}}\right) + \frac{\partial Q}{\partial q}\left(\frac{\partial q}{\partial \sigma_{ij}}\right) \quad (67)$$

From equation (66), plastic volumetric strain

$$d\varepsilon_v^p = d\varepsilon_{ii}^p = \overline{d\lambda} A_{ii} \quad (68)$$

Let us define

$$B_{ij} = \frac{\partial f}{\partial \sigma_{ij}} = \frac{\partial f}{\partial p}\left(\frac{\partial p}{\partial \sigma_{ij}}\right) + \frac{\partial f}{\partial q}\left(\frac{\partial q}{\partial \sigma_{ij}}\right) \quad (69)$$

Now, quation (64) gives us;

$$df = B_{ij} d\sigma_{ij} + \frac{\partial f}{\partial \varepsilon_v^p} d\varepsilon_v^p = 0 \quad (70)$$

The total strain increments are assumed to be the vector sum of the elastic and plastic strain increments. Using tensor algebra, it can be written;

$$d\varepsilon_{ij}^e = d\varepsilon_{ij} - d\varepsilon_{ij}^p \quad (71)$$

Using Hook's law, we can write;

$$d\sigma_{ij} = C_{ijkl}\left(d\varepsilon_{kl} - d\varepsilon_{kl}^p\right) \quad (72)$$

Now, we can get from equations (68) and (70);

$$df = B_{ij} C_{ijkl}\left(d\varepsilon_{kl} - \bar{\lambda} A_{kl}\right) + \frac{\partial f}{\partial \varepsilon_v^p} \overline{d\lambda} A_{ii} = 0 \quad (73)$$

Where the value of $\overline{d\lambda}$ is given by;

$$\overline{d\lambda} = \frac{B_{ij} C_{ijkl} d\varepsilon_{kl}}{B_{ij} C_{ijkl} A_{kl} - \frac{\partial f}{\partial \varepsilon_v^p} A_{ii}} \quad (74)$$

Now, the constitutive elastoplastic relation can be expressed in tensor format (Desai & Siriwardane, 1984);

$$d\sigma_{ij} = C_{ijkl} d\varepsilon_{kl} - \frac{C_{ijkl} A_{kl} B_{mn} C_{mnrs} d\varepsilon_{rs}}{B_{mn} C_{mnrs} A_{rs} - \frac{\partial f}{\partial \varepsilon_v^p} A_{ii}} \quad (75)$$

$$\Rightarrow d\sigma_{ij} = \left[C_{ijrs} - \frac{C_{ijkl} A_{kl} B_{mn} C_{mnrs}}{B_{mn} C_{mnrs} A_{rs} - \frac{\partial f}{\partial \varepsilon_v^p} A_{ii}}\right] d\varepsilon_{rs} \quad (76)$$

The constitutive relation presented by equation (76) is in tensor fomrat. It can be exprssed in matrix format and solved by GET.

$$\{d\sigma\} = [C^{ep}]\{d\varepsilon\} \quad (77)$$

Where C^{ep} is the elastoplastic constitutive matrix. It can be calculated using the equation;

$$[C^{ep}] = [C^e] - [C^p] \quad (78)$$

For associative flow rule, it is written;

$$\frac{\partial Q}{\partial \sigma_{ij}} = \frac{\partial f}{\partial \sigma_{ij}} \quad (79)$$

$$\Rightarrow A_{ij} = B_{ij} \quad (80)$$

Equation (80) can be written in terms of invariants;

$$A_{ij} = \frac{\partial f}{\partial I_1}\frac{\partial I_1}{\partial \sigma_{ij}} + \frac{\partial f}{\partial J_{2D}}\frac{\partial J_{2D}}{\partial \sigma_{ij}} \quad (81)$$

Differentiating equation (81) gives us;

$$A_{ij} = M^2(2I_1 - I_{10})\delta_{ij} + 27S_{ij} \quad (82)$$

where, the deviatoric stress tensor;

$$S_{ij} = \frac{\partial J_{2D}}{\partial \sigma_{ij}} = \sigma_{ij} - \frac{I_1}{3}\delta_{ij} \quad (83)$$

Now, using the chain rule of differentiation, we have

$$\frac{\partial f}{\partial \varepsilon_v^p} = \frac{\partial f}{\partial p_0}\frac{\partial p_0}{\partial \varepsilon_v^p} = -\frac{M^2 p p_0(1+e_0)}{\lambda - \kappa} \quad (84)$$

$$\frac{\partial f}{\partial \varepsilon_v^p} = -\frac{M^2 I_1 I_{10}(1+e_0)}{\lambda - \kappa} \quad (85)$$

Using equations (58), (68) and (81), we can get;

$$dI_{10} = \frac{I_{10}(1+e_0)}{\lambda - \kappa}\bar{\lambda}A_{ii} \quad (86)$$

2. THE MCC MODEL IMPLEMENTATION IN THE ISU METHOD

Our aim here is to determine the stress increment $d\sigma_{ij} = [d\sigma_{11}, d\sigma_{22}d\sigma_{33}, 0,0,0]$ at a point in clay soil corresponding to a given strain increment, i.e., $d\varepsilon_{ij} = [d\varepsilon_{11}, d\varepsilon_{22}d\varepsilon_{33}, 0,0,0]$ under isotropic triaxial strain condition. Stress increments are calculated from equation (76) using Gauss elimination technique (GET). A schematic flow chart for implementation of the MCC model using the GET is shown in Figure *10*. The model in the chapter is implemented in the ISU method. The C++ computer programming performed for implementation of the model is listed in Appendix.

2.1 INPUT PARAMETERS FOR THE MCC MODEL IMPLEMENTATION IN THE ISU METHOD

Following parameters were declared in the appendix with the C++ code for numerical implementation of the modified Cam clay.

1. **Calculation type**:

ISU and GET were employed.

2. **Material Type**:
Clay soil

3. **Yield status**:
Isotropic hardening, i.e., the yield surface expands uniformly without changing its position in the stress space.

4. **Material constants**:
EG=Bulk shear modulus
EK=Elastic bulk modulus
Lamda = slope of normal consolidation line (NCL)
M = slope of critical state line (CSL)
Kappa= slope of swelling line
I_{10} = Hardening parameter, i.e., size of the yield surface
e_0 = initial void ratio

5. **Strain increments**,

$$DE = d\varepsilon_{ij} = [d\varepsilon_{11}, d\varepsilon_{22}, d\varepsilon_{33}, 0,0,0]$$

6. **Stress state at previous step**;

$$S = \sigma_{ij}^n = [\sigma_{11}, \sigma_{22}, \sigma_{33}, 0,0,0]$$

2.2 ALGORITHM FOR IMPLEMENTATION OF THE MCC MODEL

Here, this thesis paper will outline step by step procedure with a view to implement the MCC model by incremental stress update method. A self-teaching flow chart in Figure *10* is used to do the computer coding.

Step 1: Take input quantities EG, EK, M, Lamda, Kappa, I10, e_0 , σ_{ij}^n, $d\varepsilon_{ij}$ for strain controlled simulation, $d\sigma_{ij}$ for stress controlled simulation.

Step 2: Compute C^e

Step 3. Compute $d\sigma_{ij} = C^e d\varepsilon_{ij}$ if all six components of $d\varepsilon_{ij}$ are known. But is all components of $d\sigma_{ij}$ are known, compute $d\varepsilon_{ij}$ by solving $d\sigma_{ij} = C^e d\varepsilon_{ij}$ with the application of GET.

Step 4: Compute trial stress $\sigma_{ij}^t = \sigma_{ij}^n + d\sigma_{ij}$

Step 5: Compute yield function f of the MCC model

Step 6: If $f < 0$, final stress state will be $\sigma_{ij}^{n+1} = \sigma_{ij}^t$ and go to step 8

Else $f > 0$; elasto-plastic computation is to be performed

Step 7 (a): Compute $\frac{\partial f}{\partial \sigma_{ij}}$ as given by equation (82)

Step 7(b) compute $\frac{\partial f}{\partial \sigma_{ii}}$

Step 7(c): compute $\frac{\partial f}{\partial \varepsilon_v^p}$ as given by equation (85)

Step 7(d): Compute $C_{ijkl}\frac{\partial f}{\partial \sigma_{ij}}$

Step 7(e): Compute $\frac{\partial f}{\partial \sigma_{mn}} C_{mnrs} \frac{\partial f}{\partial \sigma_{rs}}$

Step 7(f): compute $\frac{\partial f}{\partial \varepsilon_v^p}$ as given by equation (85)
Step 7(g): compute C^{ep} as given by equation (76)
Step 7(h): compute $d\sigma_{ij}^{ep} = C^{ep} d\varepsilon_{ij}$
Step 7(i): compute $\bar{\lambda}$
Step 7(j): Compute $d\varepsilon_v^p$ as given by equation (68)
Step 7(k): Update hardening parameter as given by equation (86)
Step 7(l): Update void ratio parameter as given by equation (30)
Step 8: Compute: σ_{ij}^{n+1},

ε_{ij}^{n+1}

q= deviatoric stress
ε_v = volumetric strain
shear strain, $\gamma = \varepsilon_3 - \varepsilon_1$
Step 9: Go to step 8 to generate more solutions of stresses and strains to plot stress-strain curve.

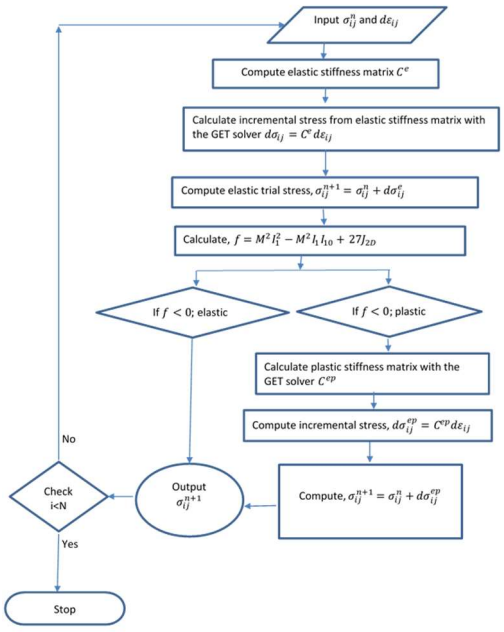

Figure 10: Flow chart for implementation of *the MCC model by incremental stress update method.*

2.4 INTERNAL VARIABLES DECLARED IN THE VISUAL C++ PROGRAM PROVIDED IN APPENDIX FOR THE ISU PROCEDURE IMPLEMENTATION

S1 = Elastic trial stress
LC = Loading condition
D1 = increment vector according to loading condition
DIJ = Kronecker delta=$\delta_{ij} = [1,1,1,0,0,0]$
DS = incremental stress = $d\sigma_{ij} = [d\sigma_{11}, d\sigma_{22} d\sigma_{33}, 0,0,0]$
I1 = First invariant of stress tensor = $\sigma_{ii} = (\sigma_{11} + \sigma_{22} + \sigma_{33})$
SD = deviatoric stress tensor = $\sigma_{ij} - \frac{1}{3} I_1 \delta_{ij}$
DFDS = Normal vector to the yield surface = $\frac{\partial Q}{\partial \sigma_{ij}} = \frac{\partial f}{\partial \sigma_{ij}}$
EM=elastic matrix= C^e
EPM = Elastoplastic matrix = C^{ep}
EMN = $C_{ijkl} \frac{\partial f}{\partial \sigma_{kl}}$
TRNEMN = $\frac{\partial f}{\partial \sigma_{mn}} C_{mnrs} \frac{\partial f}{\partial \sigma_{rs}}$
J2=second invariant of deviatoric stress tensor
DLAMDA = scalar multiplier = $\bar{\lambda}$ is defined by equation (74)
DFDEPv = $\frac{\partial f}{\partial \varepsilon_v^p}$
DEPv = $\overline{d\lambda} \frac{\partial f}{\partial \sigma_{ii}}$
Ev = volumetric strain
Es = axial strain
q = deviatoric stress = $\sqrt{3J_2}$
p= mean effective stress $p = \frac{I_1}{3}$
gamma = shear strain =$\varepsilon_3 - \varepsilon_1$
E = total strain
ε_v = volumetric strain = $\varepsilon_1 + \varepsilon_2 + \varepsilon_3$

2.5 VERIFICATION OF THE CALCULATED RESPONSE OBTAINED FROM THE ISU PROCEDURE

In the following, numerical experiments are carried out to demonstrate the performance of the ISU solution of the MCC model response. It shows the behavior of NC and OC clay in both drained and undrained isotropic triaxial compression tests. Strain controlled analyses were used in the drained and undrained compression tests. Axial and radial strain increments were input to compute stress and volumetric strain increments. Strain controlled test were used for numerical triaxial tests on NC and OC clay materials because instability occurred when strain softening took place in stress-controlled computation.

2.6 NUMERICAL TRIAXIAL TEST ON NC CLAY IN DRAINED CONDITION

In the first instance of the numerical triaxial test, the clay sample was normally consolidated in the initial isotropic pressure $\sigma_{11} = \sigma_{22} = \sigma_{33} = 200$ kPa (Figure *11*). It is assumed that the pore pressures remain equal to zero during the consolidation process. The sample is then sheared in drained conditions up to failure. Strain controlled shearing process was

implemented as the following: $\varepsilon_{11} = \varepsilon_{22} = 0;\ \varepsilon_{33} = 0.0001; \varepsilon_{12} = \varepsilon_{23} = \varepsilon_{31} = 0.$.
For numerical prediction of the behavior of NC clay under drained isotropic compression (triaxial CD test) test by the DR technique, the material properties used by the Visual C++ code given in *Table 1*. The input data were obtained from Chapter 11 of the geotechnical text book (Budhu, 2011).

Table 1: Input loading and boundary conditions used to model the stress-strain response of NC clay in drained triaxial compression test.

Material properties	Values
Soil Poisson ratio	0.3
Elastic bulk modulus, EK	10976 kPa
Bulk shear modulus, EG	4221 kPa
slope of CSL, M	0.95
slope of NCL, $\boldsymbol{\lambda}$	0.25
slope of swelling line, $\boldsymbol{\kappa}$	0.05
Initial void ratio, $\boldsymbol{e_0}$	1.15
Hardening parameter, $\boldsymbol{I_{10}}$	600 kPa
Initial stress, $\boldsymbol{\sigma_{ij}^n}$	[200, 200, 200, 0, 0, 0]
Initial strain increment, $\boldsymbol{d\varepsilon_{ij}}$	[0, 0, 0.0001, 0, 0, 0]

Stress-strain behavior predicted from the C++ coomputer program of the FE method are shown in Figure *11*. Negative volumetric strains indicate contraction of the soil mass. The ISU solutions for the soil response in numerical CD triaxial are compared with the analytical solutions presented in (Budhu, 2011). Using the soil properties *Table 1*, numerical triaxial drained test on NC clay soil was conducted in Finite Element simulation of the software PLAXIS (PLAXIS, 2016). In Figure *11*, the PLAXIS simulation results are compared with the stress-strain and stress response calculated from the ISU method and analytical method.

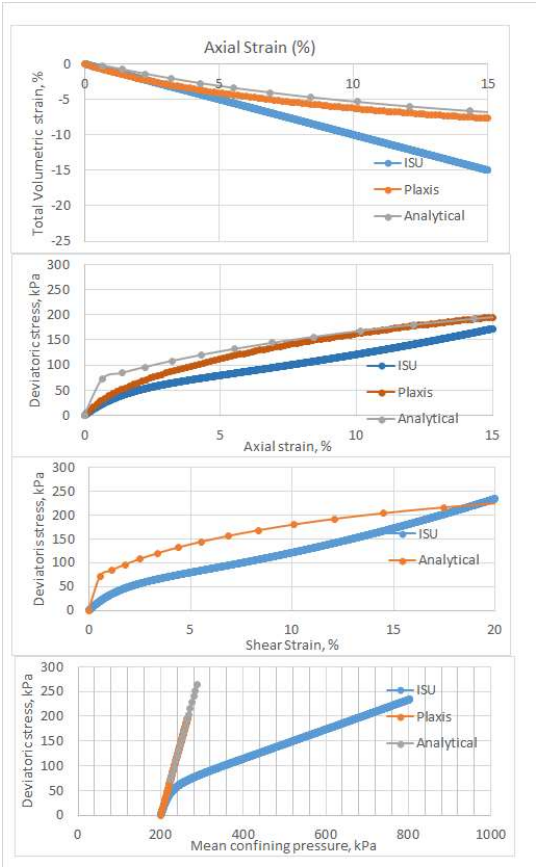

Figure 11: Numerical prediction of the behavior of NC clay in drained isotropic compression test by the ISU technique.

2.7 NUMERICAL TRIAXIAL TEST ON NC CLAY IN UNDRAINED CONDITION

In the first instance, the clay sample is normally consolidated under the initial isotropic pressure pressure $\boldsymbol{\sigma_{11} = \sigma_{22} = \sigma_{33} = 200}$ kPa(Figure 12). It is assumed that the pore pressures remains equal to zero during the consolidation process. The sample is then sheared in undrained conditions up to failure, when total elasto-plastc volume of the soil element remains equal to zero. This is implemented as the following condition: $\boldsymbol{\varepsilon_{11} = \varepsilon_{22} = -0.0005;\ \varepsilon_{33} = 0.001; \varepsilon_{12} = \varepsilon_{23} = \varepsilon_{31} = 0}$. Material properties used in the ISU method are listed in below Table 2.

Table 2: Input loading and boundary conditions used to model the stress-strain response of NC clay in undrained triaxial compression test.

Clay soil properties	Values
Soil Poisson's ratio	0.3
Elastic bulk modulus, EK	10976 kPa
Bulk shear modulus, EG	4221 kPa
Slope of CSL, M	0.95

Slope of NCL, λ	0.25
Slope of swelling line, κ	0.05
Initial void ratio, e_0	1.15
Hardening parameter, I_{10}	600 kPa
Initial isotropic stress components, σ_{ij}^{n}	[200, 200, 200, 0, 0, 0], KPa
Initial strain increment, $d\varepsilon_{ij}$	[-0.0005, -0.0005, 0.001, 0, 0, 0]

Stress-strain response predicted from the C++ code of the ISU method are shown in Figure 12. Using the soil properties ISU method are listed in below Table 2.

Table 2, numerical triaxial undrained test on NC clay soil was conducted in Finite Element simulation of the software PLAXIS (PLAXIS, 2016). In Figure 12: Response of NC clay in undrained isotropic compression test by the ISU method. Figure 12, the PLAXIS simulation results are compared with the stress-strain and stress response calculated from the ISU method and analytical method.

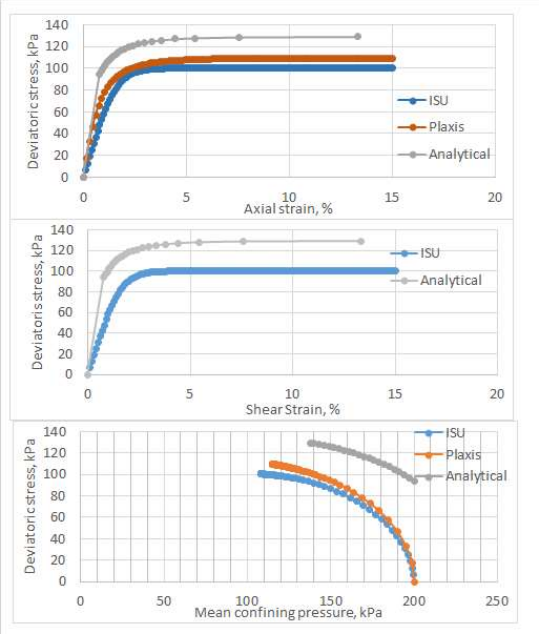

Figure 12: Response of NC clay in **undrained** isotropic compression test by the ISU method.

2.8 DISCUSSION OF NC SOIL RESPONSE CALCULATED USING ISU SIMULATION, PLAXIS SIMULATION, AND ANALYTICAL METHOD

The MCC model was numerically implemented by ISU simulation, PLAXIS simulation, and Analytical method. Stresses and strains in the soil element noted from the computed results for NC drained clay are summarized in Table 3.

Table 3: Analytical method, PLAXIS Triaxial test simulation and ISU simulation comparison for NC soil in drained condition.

Soil response curve **Figure 11**	**Prediction by analytical method**	**Prediction by ISU method**	**Prediction by PLAXIS FE simulation**
Volumetric strain versus Axial strain	7% volume contraction at 15% axial strain	15% volume contraction at 15% axial strain	7.5% volume contraction at 15 % axial strain
q versus γ (deviatoric stress versus axial strain)	Ultimate Deviatoric stress = 200 kPa at 15% axial strain,	Ultimate Deviatoric stress = 175 kPa at 15 % axial strain	Ultimate Deviatoric stress = 200 kPa at % axial strain
q versus γ (deviatoric stress versus shear strain)	Ultimate deviatoric stress capacity = 227 kPa at 20 % shear strain	Ultimate deviatoric stress capacity = 234 kPa is also at 20 % shear strain	Not calculated
q versus p (stress path)	Ultimate Deviatoric stress = 280 kPa at mean effective confining stress = 260 kPa	Ultimate Deviatoric stress = 234 kPa at mean effective confining stress = 803 kPa	Ultimate Deviatoric stress = 195 kPa at mean effective confining stress = 265 kPa

From Figure *11*, it is noted that the ISU wants to follow the PLAXIS and analytical solution of stress strain behavior as fast possible. This happens because plastic slope of the ISU solution curve has steep slope. It is evident that after a large number of increments in strain, the approximate solution from the ISU method diverges from analytical solution. It is noted from the slope (dq/dp) of the drained stress path (q versus p) shown in Figure *11* that the analytical solution reaches the CSL faster than FE solution and analytical method.

It is noted in Figure 12 that, deviatoric stress versus axial strain relation computed by the ISU method compares well with the analytical and PLAXIS results for NC clay in undrained numerical triaxial test. The numerical stress and strain response of the NC clay in undrained condition are summarized in Table 4.

Table 4: Analytical method, PLAXIS Triaxial test simulation and ISU simulation comparison for NC soil in undrained condition.

Soil response curve **Figure 12**	**Prediction by analytical method**	**Prediction by ISU method**	**Prediction by PLAXIS FE simulation**
q versus γ (deviatoric stress versus axial strain)	Ultimate Deviatoric stress = 135 kPa at 12.5% axial strain,	Ultimate Deviatoric stress = 100 kPa at 10 % axial strain	Ultimate Deviatoric stress = 110 kPa at 10 axial strain
q versus γ (deviatoric stress versus shear strain)	Ultimate deviatoric stress capacity = 130 kPa at 12.5 % shear strain	Ultimate deviatoric stress capacity = 100 kPa is also at 12.5 % shear strain	Not calculated
q versus p (stress path)	Ultimate Deviatoric stress = 130 kPa at mean effective confining stress = 143 kPa	Ultimate Deviatoric stress = 100 kPa at mean effective confining stress = 110 kPa	Ultimate Deviatoric stress = 110 kPa at mean effective confining stress = 120 kPa

The stress path in Figure 12 shows that the mean confining stress decreases from 200 kPa to 143 kPa, 110 kPa, and 120 kPa in analytical, ISU and PLAXIS analysis, respectively. This happens due to increase in excess pore water pressure in the saturated consolidated soil during deviatoric load application. The stress paths computed from the ISU and PLAXIS triaxial undrained tests compare very well. In all three approach of numerical tests: analytical, ISU and PLAXIS methods, the deviatoric stress is reduced relative to the drained case (Figure *11*). The stress path in Figure 12 shows a typical undrained response that reaches to the CSL line after moving away from the drained path shown in Figure *11*.

The implemented C++ computer program algorithm simulated both drained and undrained triaxial compression tests under the strain controlled conditions. The implemented ISU method employs back substitution of the Gaussian elimination technique to determine stress increments from a linear system of equations in a finite number of steps. The elasto-plastic stiffness matrix which connects stress and strain increments within this linear system of equations was updated at the beginning of each strain increment. Due to the large number of strain increments, the numerical ISU solution began to diverge from the analytical closed form solutions in the undrained case. In contrast, the PLAXIS solution utilizes an iterative convergence criterion to achieve the analytical solution.

CONCLUSION

The MCC numerical prediction of the stress-strain behavior of the NC and OC soil was implemented in the ISU approach. The MCC plasticity model's stress-strain equations were solved using the GET in the ISU method. Analytical solution and predicted stress-strain behavior of NC in both drained and undrained triaxilly consolidated soil were compared. There was a satisfactory level of agreement between the analytical and numerical solutions. Elasto-plastic stiffness in linear stress update procedure of the ISU method are not as effcient as the PLAXIS FE simulation. Stress-strain response computed from the ISU method diverges from the analytical response of soil due to the rapid linear approximation of the soil stiffness in the plastic zone.

The hard reality is that, due to a lack of financing for scientific study, many geotechnical stress-strain problems that arise in the real world frequently remain unsolved in our scientific labs. It is feasible to predict with a high degree of precision how the clay soil will respond to both static and dynamic loads using numerical modeling. Such modeling requires understanding of mathematics and computer programming ability (Wood, 1991). Therefore, this study encourages future geotechnical engineers to use their knowledge of coding to simulate the response of geomaterials to various boundary and loading conditions.

DECLARATION OF COMPETING INTEREST

The author declare that he has no known competing financial interests or personal relationships that could have appeared to influence the work reported in this paper.

REFERENCES

[1] Borja, R. I. (1991). Cam-Clay plasticity, Part II: Implicit integration of constitutive equation based on a nonlinear elastic stress predictor. Computer Methods in Applied Mechanics and Engineering, 225-240. Retrieved from https://doi.org/10.1016/0045-7825(91)90256-6.

[2] Budhu, M. (2011). Soil Mehcanics and Foundations. John Wiley & Sons, Inc.

[3] Cassel, A. C., Kinsey, P. J., & Sefton, D. J. (1968). Cylindrical shell analysis by Dynamic Relaxation. Proceedings of the Institution of Civil Engineers, 75-84. doi:https://doi.org/10.1680/iicep.1968.8109

[4] Chen, W. F., & Mizuno, E. (1990). Nonlinear Analysis in Soil Mechanics: Theory and Implementation. Elsevier Science.

[5] Desai, C. S., & Siriwardane, J. H. (1984). Constitutive laws for engineering materials: With emphasis on geologic materials. New Jersey 07632: Prentice-Hall, Inc., Englewood Cliffs. Retrieved from https://doi.org/10.1002/nag.1610080310

[6] Hashiguchi, K., Saitoh, K., & Okayasu, T. (2002). Evaluation of typical conventional and unconventional plasticity models for prediction of softening behaviour of soils. Geotechnique 52 (8), 561-578, 561-578. doi:https://doi.org/10.1680/geot.2002.52.8.561

[7] Irons, B., & Ahmad, S. (1984). Techniques of Finite Elements. the University of Michigan.

[8] Lambe, T. W., & Whitman, R. V. (1969). Soil Mechanics. Wiley.

[9] Ortiz, M., & Martin, J. B. (1989). Symmetry-preserving return mapping algorithms and incrementally extremal paths: A unification of concepts. International Journal for Numerical Methods in Engineering, 1839-1853. doi:10.1002/nme.1620280810

[10] Otter, J. R. (1966). Dynamic relaxation compared with other iterative finite difference methods. Nuclear Engineering and Design, 183-185. doi:https://doi.org/10.1016/0029-5493(66)90157-9

[11] PLAXIS. (2016). PLAXIS Reference Manual. Bentley Systems Inc.

[12] Riks, E. (1979). An incremental approach to the solution of snapping and buckling problems. International Journal of Solids and Structures, 529-551. doi:https://doi.org/10.1016/0020-7683(79)90081-7

[13] Roscoe, K. H. (1970). The Influence of Strains in Soil Mechanics. Géotechnique. Retrieved from https://doi.org/10.1680/geot.1970.20.2.129

[14] Roscoe, K. H., Schofield, A. N., & Wroth, C. P. (1958). On the Yielding of Soils. Géotechnique, 22-53. doi:http://doi.org/10.1680/geot.1958.8.1.22

[15] Siddiquee, M. S., Tanaka, T., & Tatsuoka, F. (1995). Tracing the equilibrium path by dynamic relaxation in materially nonlinear problems. International journal for numerical and analytical methods. doi:https://doi.org/10.1002/nag.1610191102

[16] Simo, J. C., & Taylor, R. (1986). A return mapping algorithm for plane stress elastoplasticit. https://doi.org/10.1002/nme.1620220310. doi:https://doi.org/10.1002/nme.1620220310

[17] Wood, d. M. (1991). Soil Behaviour and Critical State Soil Mechanics. Cambridge University Press. doi:https://doi.org/10.1017/CBO9781139878272

[18] Zienkiewicz, O. C., Taylor, R. L., & Zhu, J. Z. (2013). The Finite Element Method: Its Basis and Fundamentals. Elsevier Ltd. Retrieved from https://doi.org/10.1016/C2009-0-24909-9

APPENDIX

The C++ computer program is presented for the ISU method for numerical triaxial test simulation of the MCC model.

// C++ programming for source code for implementing the MCC model in the ISU method

```
#include<iostream>
#include<math.h>
#include<fstream>
int main()
{double S[6],S1[6],E[6],LC[6],DI[6];
double DIJ[6],DS[6],DE[6],SD[6],DEPv;
double DFDS[6],EM[6][6],EPM[6][6],EMN[6];
double TRNEMN,LAMDA,KAPPA;
double p,q,I1o,DLAMDA,e,M,Aii,I1,J2,gama,f;
double DFDEPv;
double EK,EG,EM1,EM2,EM3;
double y;
int i,j,k,n,count=0;
  //The variable 'gama' keeps the values of shear strain and prints
  them in the gama.text file. The //variable 'pout' keeps the values
  of mean effective stress p and prints the in the pout.txt file. The
  //variable 'qout' keeps the values of q and prints them in them
  qout.txt file. The variable Evout keeps //the values of volumetric
  strain and prints them in Evout.txt file. The variable Eaout keeps
  the values //of axial strain and prints them in Eaout.txt file.
std::ofstream gamaout("gama.txt");
std::ofstream pout("p.txt");
std::ofstream qout("q.txt");
std::ofstream Evout("Ev.txt");
std::ofstream Eaout("Ea.txt");
EG=4221,EK=10976,M=0.95,LAMDA=.25,KAPPA=.05,e=1.15,I1o
=600;
// Cell pressures: sigma2, sigma2, sigma3
   for(i=0;i<6;i++){
      if(i<3)S[i]=200;
      else S[i]=.0;
   }
   for (i=0;i<=6;i++)
      E[i]=.0; DIJ[0]=1; DIJ[1]=1; DIJ[2]=1; DIJ[3]=0;
      DIJ[4]=0; DIJ[5]=0;
      do{
         EM1=EK+4/3*EG;
         EM2=EK-2/3*EG;
         EM3=EG;
         for(i=0;i<6;i++)
            for(j=0;j<6;j++) EM[i][j]=0;
            EM[0][0]=EM[1][1]=EM[2][2]=EM1;
            EM[3][3]=EM[4][4]=EM[5][5]=EM3;

EM[0][1]=EM[0][2]=EM[1][0]=EM[1][2]=EM[2][0]=EM[2][1]=EM2;
  //Appropriate loading condition LC and corresponding increment
  DI is given. // This listing of the ISU method simulates isotropic
  consolidated undrained (CIU) test where change in //volumetric
  strain is zero. LC=1.0 means strain increment is provided and
  LC=0.0 means stress //increment must be provided.
            LC[0]=1;DI[0]=0;
            LC[1]=1;DI[1]=0;
            LC[2]=1;DI[2]=0.0001;
            LC[3]=0;DI[3]=0;
            LC[4]=0;DI[4]=0;
            LC[5]=0;DI[5]=0;
                  for(i=0;i<6;i++){
            if(LC[i]==0){
                  DS[i]=DI[i];
                  DE[i]=0;
            }
            else {
                  DS[i]=0;
                  DE[i]=DI[i];
            }
         }
         for(i=0;i<6;i++){
               if(LC[i]==1){
                     for(j=0;j<6;j++)
                           if(LC[j]==0)DS[j]-=EM[i][j]*DE[i];
               }
         }
         for(k=0;k<5;k++){
               if(LC[k]==0){
                     for(i=k+1;i<6;i++){
                           if(LC[i]==0){
                                 y=EM[i][k]/EM[k][k];
                                 for(j=k;j<6;j++)
                                       if(LC[j]==0)EM[i][j]-=y*EM[k][j];
                           }
                     }
               }
         }

         for(i=0;i<6;i++)
               if(LC[i]==0)n=i;
               DE[n]=DS[n]/EM[n][n];
               for(i=n-1;i>=0;i--){
                     if(LC[i]==0){
                           y=DS[i];
                           for(j=i+1;j<=n;j++)
                                 if(LC[j]==0)y-=EM[i][j]*DE[j];
                                 DE[i]=y/EM[i][i];
                     }
               }
               for(i=0;i<6;i++){
                     if(LC[i]==1){
                           DS[i]=0;
                           for(j=0;j<6;j++)DS[i]+=EM[i][j]*DE[j];
                     }
               }
               for(i=0;i<6;i++)
                     if(LC[i]==0) DS[i]=DI[i];
                     for(i=0;i<6;i++)
                           S1[i]=S[i]+DS[i];
                     for(i=0;i<6;i++)
std::cout<<"S1["<<i+1<<"]::"<<S1[i]<<std::endl;
                  I1=(S1[0]+S1[1]+S1[2]);
                  for(i=0;i<6;i++)
                        SD[i]=S1[i]-(I1*DIJ[i])/3;
                        J2=(((S1[0]-S1[1])*(S1[0]-S1[1])+(S1[1]-
S1[2])*(S1[1]-S1[2])+(S1[2]-S1[0])*(S1[2]-
S1[0]))/6)+S1[3]*S1[3]+S1[4]*S1[4]+S1[5]*S1[5];
                        f=M*M*I1*I1-M*M*I1*I1o+27*J2;
                        if(f>0){
                              std::cout<<"It is now Elasto-plastic
state"<<std::endl;
                              EM1=EK+4/3*EG;
                              EM2=EK-2/3*EG;
                              EM3=EG;
                              for(i=0;i<6;i++)
                              for(j=0;j<6;j++) EM[i][j]=0;
                              EM[0][0]=EM[1][1]=EM[2][2]=EM1;
EM[3][3]=EM[4][4]=EM[5][5]=EM3;
EM[0][1]=EM[0][2]=EM[1][0]=EM[1][2]=EM[2][0]=EM[2][1]=EM2;
                              for(i=0;i<6;i++)
                              DFDS[i]=M*M*(2*I1-
I1o)*DIJ[i]+27*SD[i];
Aii=(DFDS[0]+DFDS[1]+DFDS[2]);
                              TRNEMN=0;
                              for(i=0;i<6;i++){
                                    EMN[i]=0;
                                    for(j=0;j<6;j++)
EMN[i]+=EM[i][j]*DFDS[j];
TRNEMN+=EMN[i]*DFDS[i];
                              }
                        DFDEPv=-(M*M*I1*I1o*(1+e)/(LAMDA-
KAPPA));
                        for(i=0;i<6;i++)
                              for(j=0;j<6;j++)
                                    EPM[i][j]=EM[i][j]-
(EMN[i]*EMN[j])/(TRNEMN-DFDEPv*Aii);
                                    for(i=0;i<6;i++){
                                          if(LC[i]==0){
                                                DS[i]=DI[i];
                                                DE[i]=0;
                                          }
                                          else{
                                             DS[i]=0;
                                             DE[i]=DI[i];
                                          }
                                    }
                                    for(i=0;i<6;i++){
                                          if(LC[i]==1){
for(j=0;j<6;j++)
                                                if(LC[j]==0)      DS[j]-
=EPM[j][i]*DE[i];
                                          }
                                    }
                                    for(k=0;k<5;k++){
                                       if(LC[k]==0){
for(i=k+1;i<6;i++){
```

```
                                                    if(LC[i]==0){
y=EPM[i][k]/EPM[k][k];
for(j=k;j<6;j++)
if(LC[j]==0)
EPM[i][j]-=y*EPM[k][j];
DS[i]-=y*DS[k];
                                                    }
                                                }
                                            }
                                        }
                                        for(i=0;i<6;i++)
                                            if(LC[i]==0) n=i;
DE[n]=DS[n]/EPM[n][n];
                                        for(i=n-1;i>=0;i--){
                                            if(LC[i]==0){
                                                y=DS[i];
for(j=i+1;j<=n;j++)
if(LC[j]==0)
y-=EPM[i][j]*DE[j];
DE[i]=y/EPM[i][i];
                                            }
                                        }
                                        for(i=0;i<6;i++){
                                            if(LC[i]==1){
                                                DS[i]=0;
for(j=0;j<6;j++) DS[i]+=EPM[i][j]*DE[j];
                                            }
                                        }

                                        for(i=0;i<6;i++)
if(LC[i]==0)DS[i]=DI[i];
                                            DLAMDA=0;
                                            for(i=0;i<6;i++)
DLAMDA+=(EMN[i]*DE[i])/(TRNEMN-DFDEPv*Aii);
DEPv=DLAMDA*Aii;
//del_I10=?
I1o+=I1o*(1+e)*DEPv/(LAMDA-KAPPA);
e-=(1+e)*(DE[0]+DE[1]+DE[2]);
                                }
                                for(i=0;i<6;i++){
                                    S[i]+=DS[i];
                                    E[i]+=DE[i];
                                }
                                I1=(S[0]+S[1]+S[2]);
                                for(i=0;i<6;i++)
                                    SD[i]=S[i]-(I1*DIJ[i])/3;
                                    J2=(((S[0]-S[1])*(S[0]-S[1])+(S[1]-
S[2])*(S[1]-S[2])+(S[2]-S[0])*(S[2]-
S[0]))/6)+S[3]*S[3]+S[4]*S[4]+S[5]*S[5];
                                    p=I1/3; q=sqrt(3*J2); gama=E[2]-E[0];
                                    std::cout<<std::endl;
                                    for(i=0;i<6;i++)
std::cout<<std::endl<<"S["<<i+1<<"]::"<<S[i];
                                    std::cout<<std::endl;
                                    for(i=0;i<6;i++)
std::cout<<std::endl<<"E["<<i+1<<"]::"<<E[i];
std::cout<<"I1o::"<<I1o<<std::endl; std::cout<<"2*I1::"<<2*I1;
gamaout<<gama*100<<std::endl; pout<<p<<std::endl;
 qout<<q<<std::endl;
 Evout<<-(E[0]+E[1]+E[2])*100<<std::endl;
Eaout<<E[2]*100<<std::endl; count++;
      }
while(count<=2000); gamaout.close(); pout.close();
   qout.close();
   Evout.close();
   Eaout.close();

}
```